Multiwavelength emission from the periodic X-ray binary LS I $+61^{\circ}303$

Frédéric Jaron

Department of Geodesy and Geoinformation, TU Wien, Austria
Max-Planck-Institut für Radioastronomie, Bonn, Germany

Department of Astrophysics Seminar
University of Vienna
March 24, 2023

Max-Planck-Institut für Radioastronomie

MAX-PLANCK-GESELLSCHAFT

TECHNISCHE UNIVERSITÄT WIEN

1. Introduction
   - Electromagnetic spectrum
   - Very high energy gamma-rays
   - X-ray binary
   - The binary star LS I $+61°303$
   - Variability and periodicities
2. The super-orbital modulation of LS I $+61°303$
3. Physical scenario
4. Conclusion and outlook

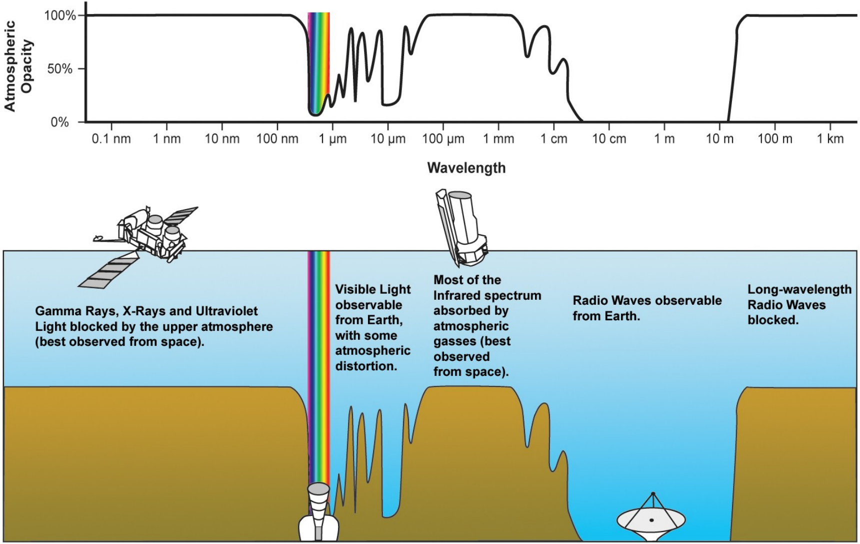
Atmospheric Opacity
100%
50%
0%
0.1 nm
1 nm
10 nm
100 nm
1 µm
10 µm
100 µm
1 mm
1 cm
10 cm
1 m
10 m
100 m
1 km
Wavelength
Gamma Rays, X-Rays and Ultraviolet Light blocked by the upper atmosphere (best observed from space).
Visible Light observable from Earth, with some atmospheric distortion.
Most of the Infrared spectrum absorbed by atmospheric gasses (best observed from space).
Radio Waves observable from Earth.
Long-wavelength Radio Waves blocked.

Credit: NASA

Cherenkov telescopes of the MAGIC observatory (La Palma).

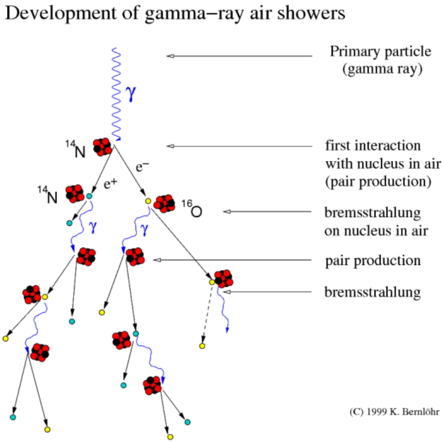

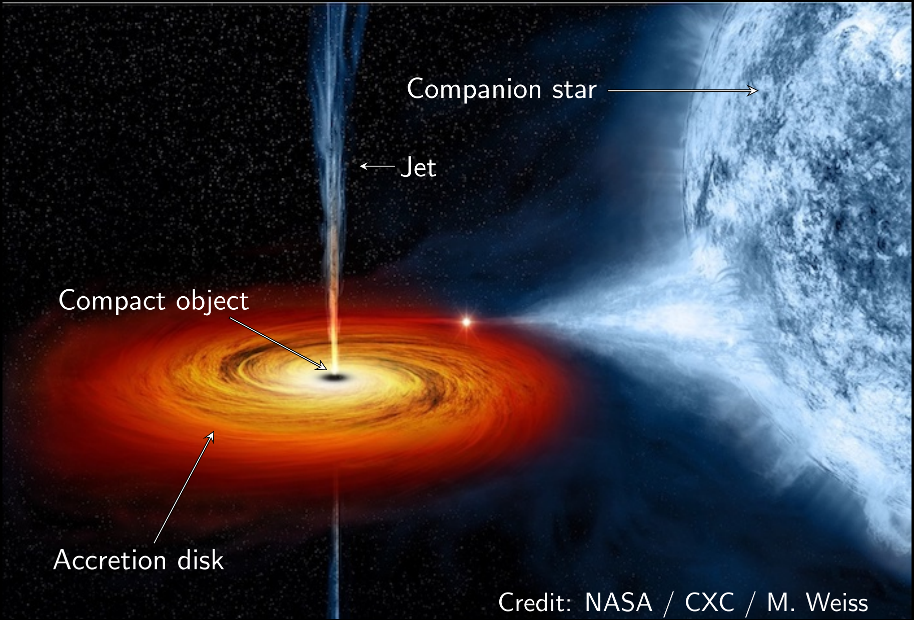
Companion star
Jet
Compact object
Accretion disk
Credit: NASA / CXC / M. Weiss

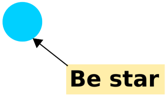
Be star

$$\rho(r) = \rho_0 \left(\frac{r}{R_*}\right)^{-n}, \ n = 3.25$$

(Martí & Paredes 1995)

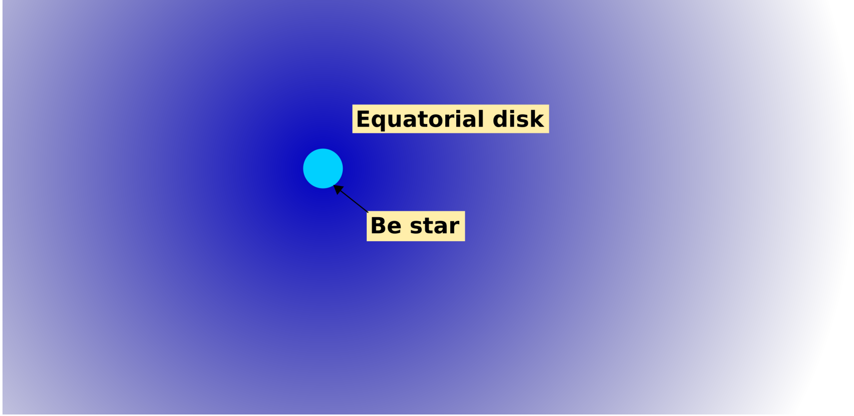

$$\rho(r) = \rho_0 \left(\frac{r}{R_*}\right)^{-n}, \quad n = 3.25$$

(Martí & Paredes 1995)

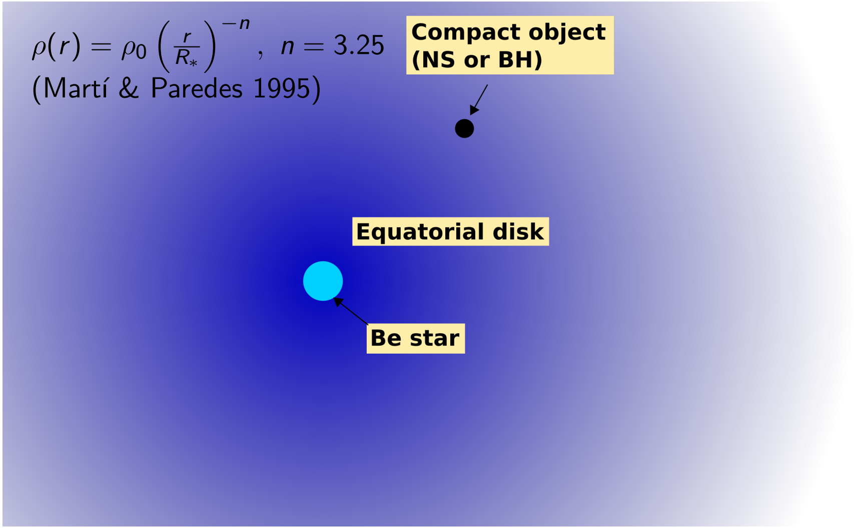

$$\rho(r) = \rho_0 \left(\frac{r}{R_*}\right)^{-n}, \quad n = 3.25$$

(Martí & Paredes 1995)

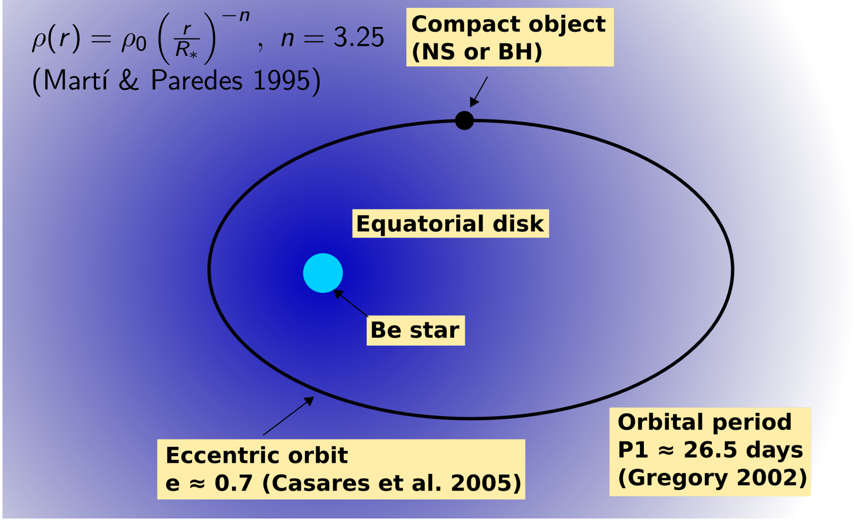

Orbital phase $\Phi = \frac{t-t_0}{P_1} - \text{int}\left(\frac{t-t_0}{P_1}\right)$

Variability and periodicities in the emission from LS I $+61^{\circ}303$

Variability and periodicities in the emission from LS I $+61^{\circ}303$

1. Short-term variability

Micro-flaring activity, sometimes (quasi) periodic on time scales of hours

Sharma *et al.* (2021) ; Nösel *et al.* (2018) ; Jaron *et al.* (2017) ; Peracaula *et al.* (1997).

Var

1. S
Mic
Sha

Short-term variability (Example)

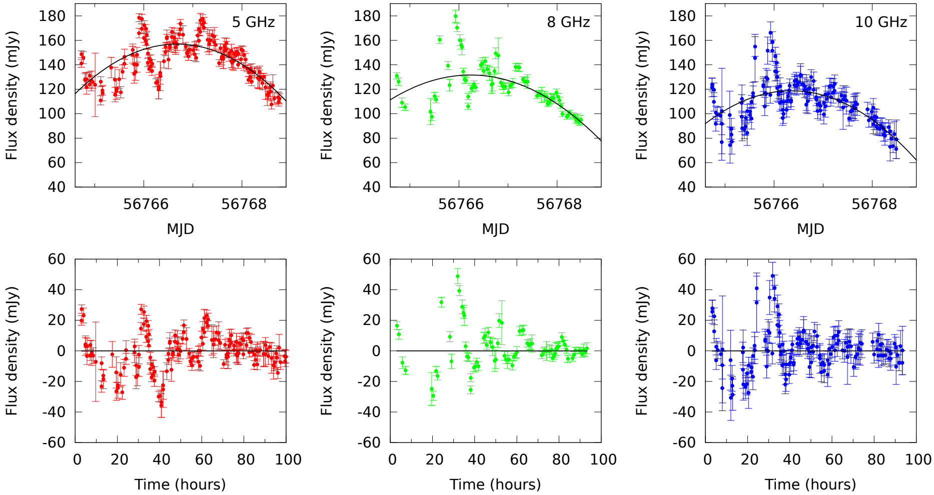

Observations with the 100-m Radio Telescope Effelsberg (Germany) Jaron *et al.* (2017, MNRAS)

Variability and periodicities in the emission from LS I $+61^{\circ}303$

1. Short-term variability

Micro-flaring activity, sometimes (quasi) periodic on time scales of hours
Sharma *et al.* (2021) ; Nösel *et al.* (2018) ; Jaron *et al.* (2017) ; Peracaula *et al.* (1997).

2. Orbital periodicity

Regular outbursts occur related to the orbital period
$P_1 = 26.4960 \pm 0.0028$ days Gregory 2002, ApJ, 575, 1
Occurrence of radio outbursts is precisely predictable Jaron & Massi 2013, A&A, 559, A129.

Variability an 3

1. Short-term va
Micro-flaring act
Sharma *et al.* (2 *al.* (1997).

2. Orbital perioc
Regular outburst
$P_1 = 26.4960 \pm$
Occurrence of ra A, 559, A129.

Regular radio outbursts

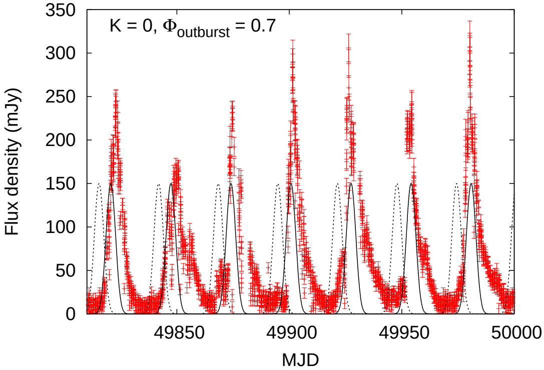

Zoom into Green Bank Interferometer monitoring (8 GHz)

Jaron & Massi (2013, A&A)

Variability and periodicities in the emission from LS I $+61°303$

1. Short-term variability

Micro-flaring activity, sometimes (quasi) periodic on time scales of hours

Sharma *et al.* (2021) ; Nösel *et al.* (2018) ; Jaron *et al.* (2017) ; Peracaula *et al.* (1997).

2. Orbital periodicity

Regular outbursts occur related to the orbital period

$P_1 = 26.4960 \pm 0.0028$ days Gregory 2002, ApJ, 575, 1

Occurrence of radio outbursts is precisely predictable Jaron & Massi 2013, A&A, 559, A129.

3. Long-term (super-orbital) modulation

$P_{\text{long}} = 1667 \pm 8$ days ≈ 4.6 years Gregory 2002, ApJ, 575, 1

Variab

1. Sho
Micro-f
Sharma 7).

2. Orbi
Regula
$P_1 = 2$
Occurr A129.

3. Lon
$P_{\text{long}} =$

Long-term modulation

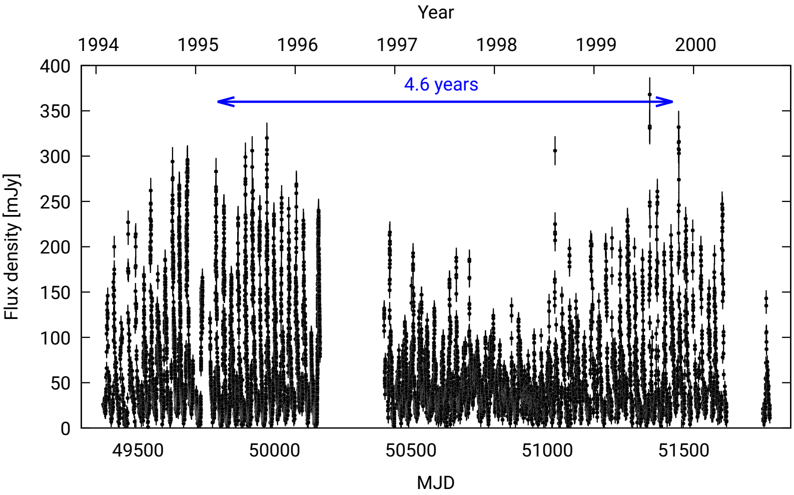

Green Bank Interferometer monitoring (8 GHz)

Variability and periodicities in the emission from LS I $+61^{\circ}303$

1. Short-term variability

Micro-flaring activity, sometimes (quasi) periodic on time scales of hours

Sharma *et al.* (2021) ; Nösel *et al.* (2018) ; Jaron *et al.* (2017) ; Peracaula *et al.* (1997).

2. Orbital periodicity

Regular outbursts occur related to the orbital period

$P_1 = 26.4960 \pm 0.0028$ days Gregory 2002, ApJ, 575, 1

Occurrence of radio outbursts is precisely predictable Jaron & Massi 2013, A&A, 559, A129.

3. Long-term (super-orbital) modulation

$P_{\mathrm{long}} = 1667 \pm 8$ days ≈ 4.6 years Gregory 2002, ApJ, 575, 1

Subject of this talk: Behavior of this long-term modulation across the EM spectrum.

Variability and periodicities in the emission from LS I $+61^{\circ}303$

1. Short-term variability

Micro-flaring activity, sometimes (quasi) periodic on time scales of hours

Sharma *et al.* (2021) ; Nösel *et al.* (2018) ; Jaron *et al.* (2017) ; Peracaula *et al.* (1997).

2. Orbital periodicity

Regular outbursts occur related to the orbital period

$P_1 = 26.4960 \pm 0.0028\,\mathrm{days}$ Gregory 2002, ApJ, 575, 1

Occurrence of radio outbursts is precisely predictable Jaron & Massi 2013, A&A, 559, A129.

3. Long-term (super-orbital) modulation

$P_{\mathrm{long}} = 1667 \pm 8\,\mathrm{days} \approx 4.6\,\mathrm{years}$ Gregory 2002, ApJ, 575, 1

Subject of this talk: Behavior of this long-term modulation across the EM spectrum.

Long-term phase: $\Theta = \frac{t-T_0}{P_{\mathrm{long}}} - \mathrm{int}\left(\frac{t-T_0}{P_{\mathrm{long}}}\right) \in [0,1)$

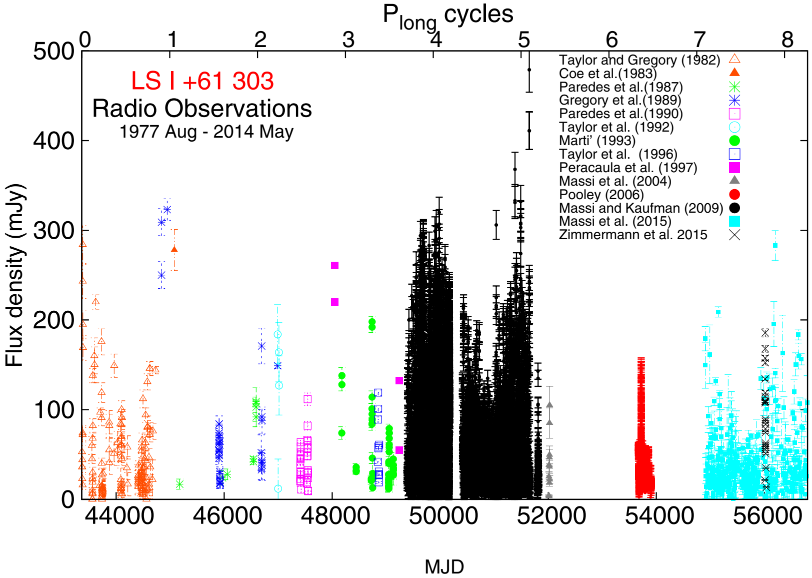

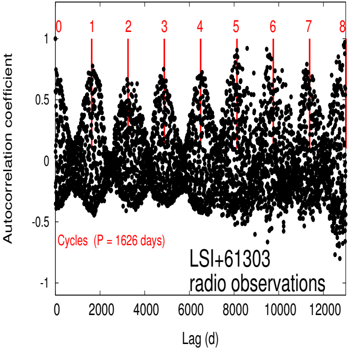

Massi & Torricelli-Ciamponi 2016, A&A, 585, A123 → and ongoing Jaron *et al.* 2018, MNRAS, 478, 1

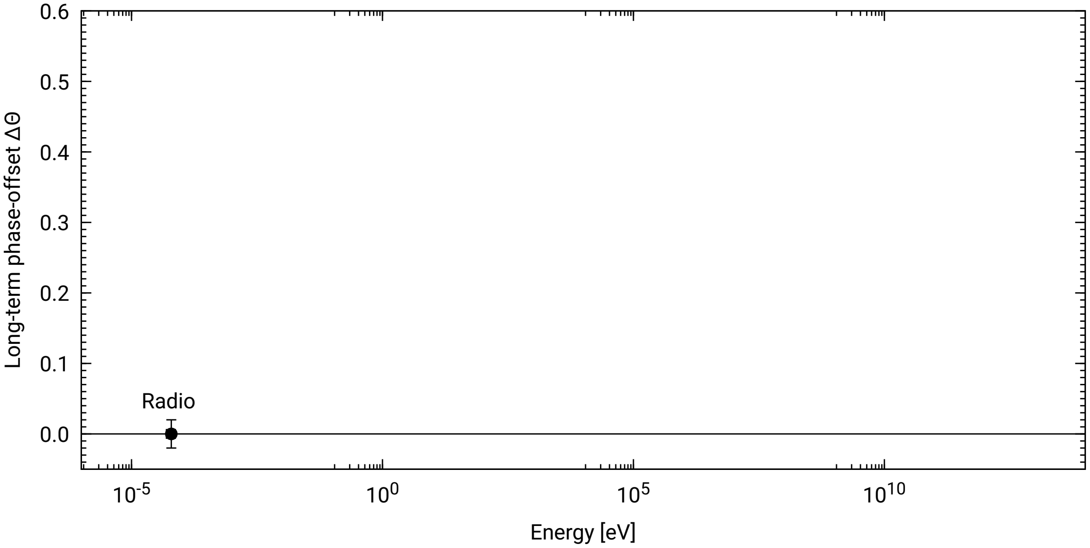

Jaron, Universe 2021, 7(7), 245

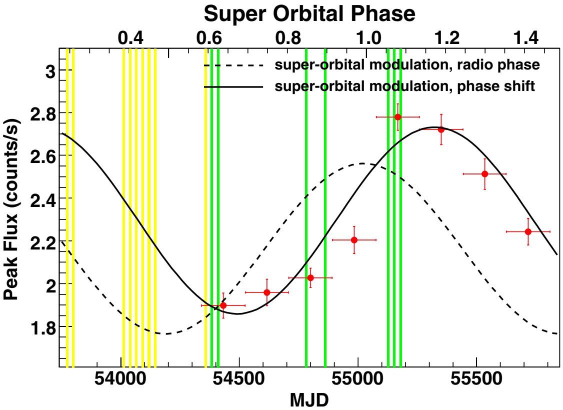

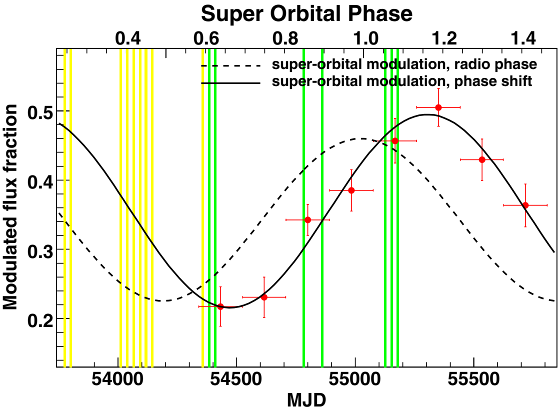

Figure 1 in Li *et al.* (2012)

⇒ Phase offset between X-rays and radio: $\Delta\Theta = 0.17 \pm 0.03$

Li *et al.* 2012, ApJL, 744, 1, L13

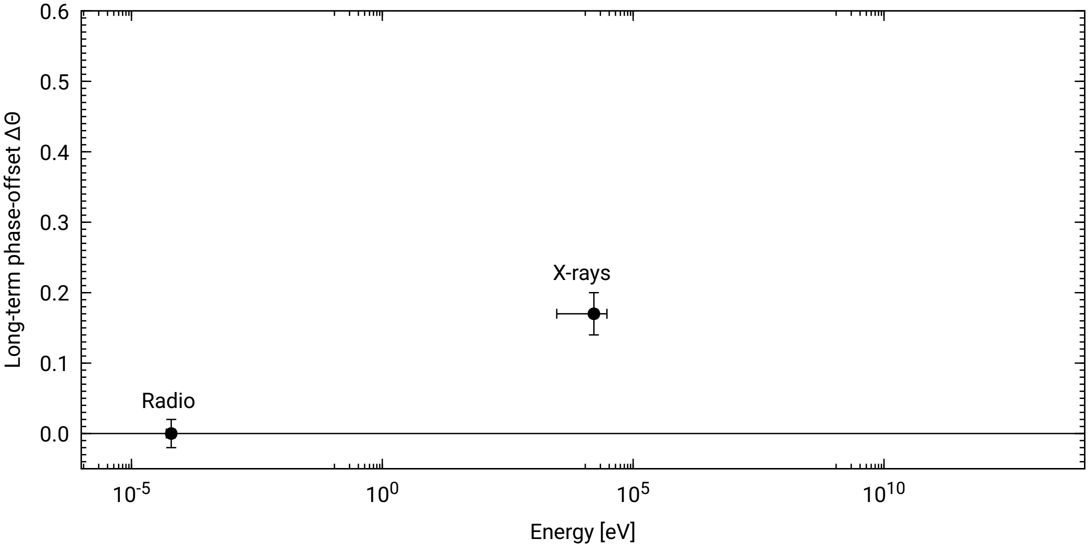

Jaron, Universe 2021, 7(7), 245

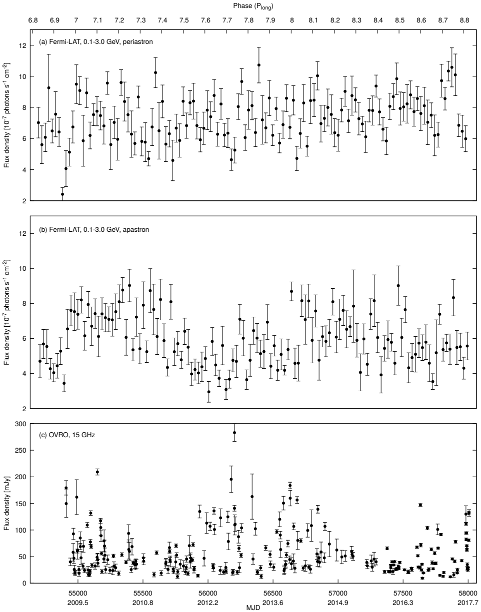

Long-term modulation profiles

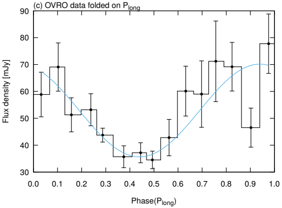

Radio

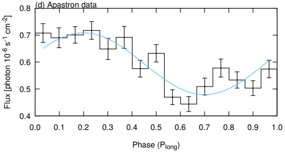

Gamma-rays

$\Rightarrow$ Phase-offset between GeV and radio:
$\Delta\Theta = 0.26 \pm 0.03$

Jaron *et al.* 2018, MNRAS, 478, 1

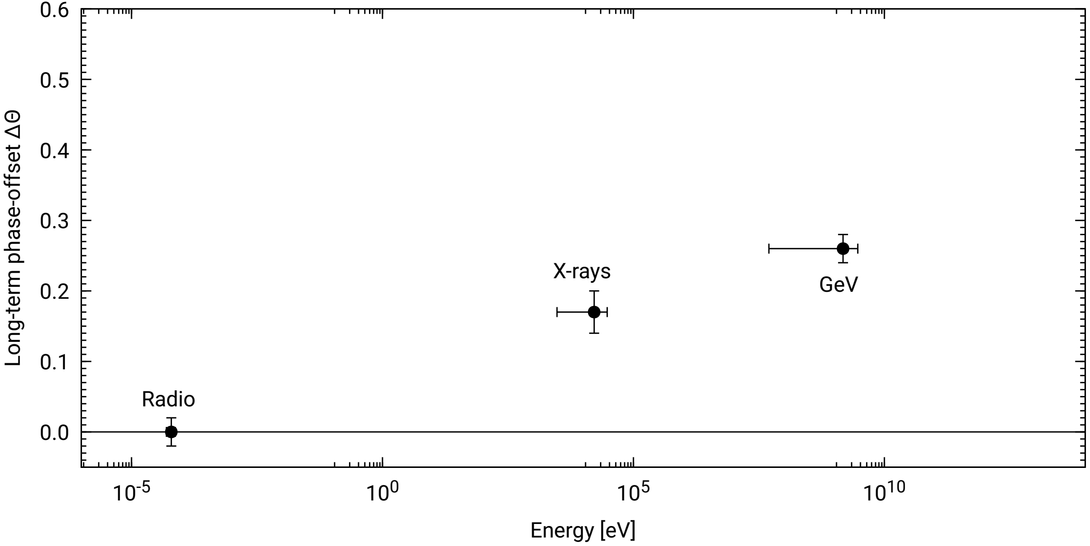

Jaron, Universe 2021, 7(7), 245

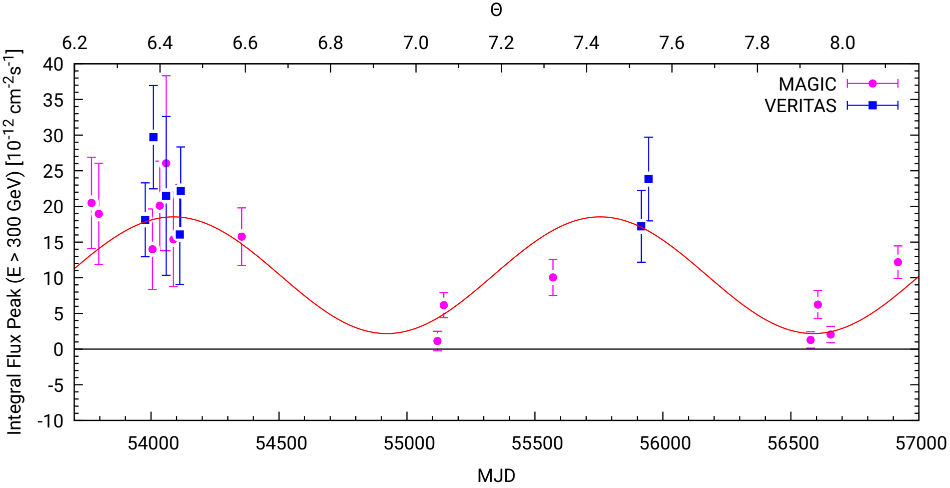

$\Rightarrow$ Phase-offset between TeV and radio: $\Delta\Theta = 0.51 \pm 0.03$

Ahnen *et al.* 2016, A&A, 591, A76 ; Jaron, Universe 2021, 7(7), 245

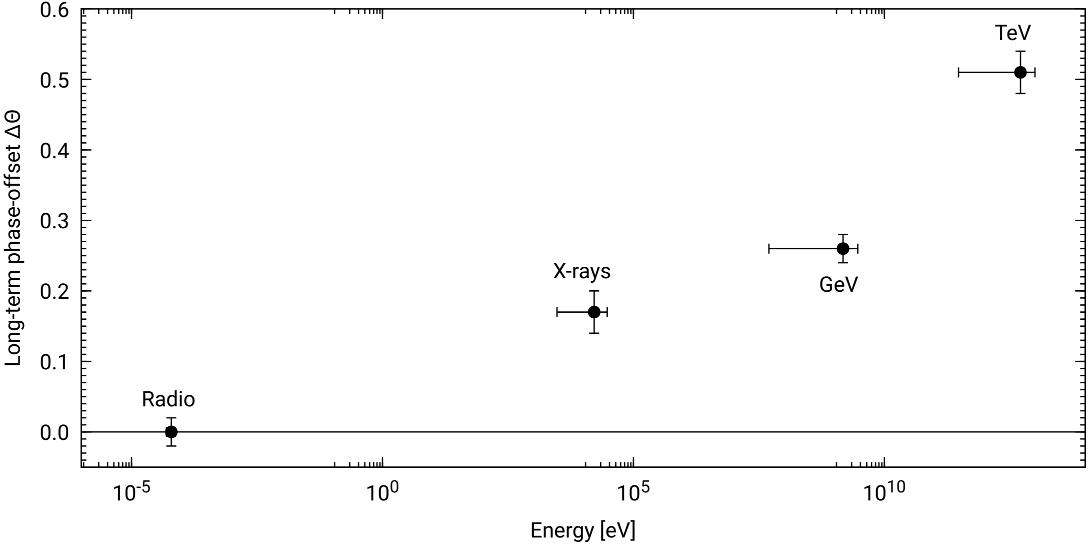

Jaron, Universe 2021, 7(7), 245

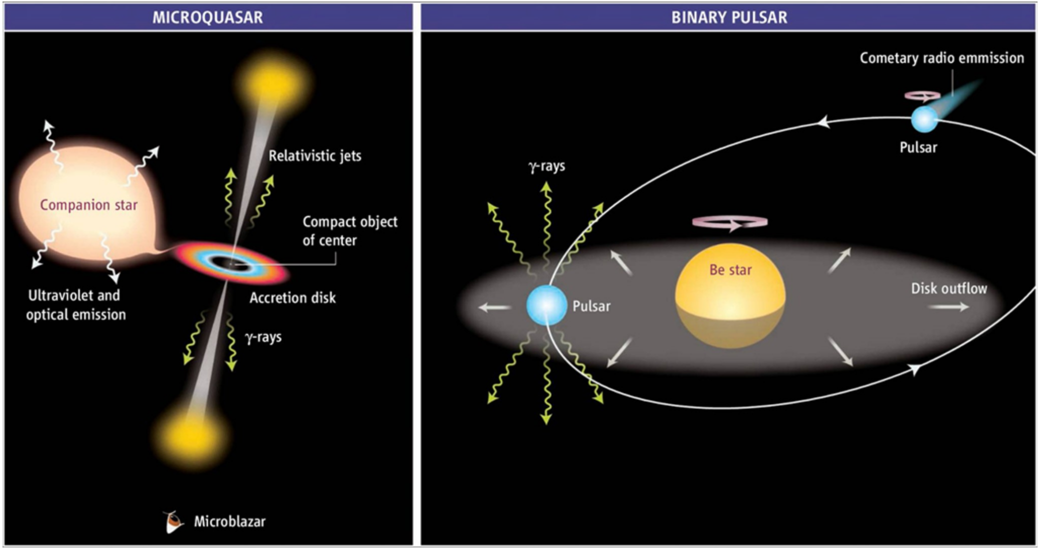

Mirabel (2006, Science)

What is the physical reason for the long-term modulation in LS I +61°303?

1. Changes in the Be star disk?

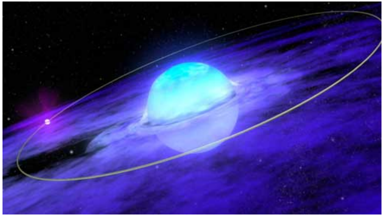

Credit: Walt Feimer, NASA/GFSC

First suggested by Gregory *et al.* (1989)

Still discussed (see Chernyakova *et al.* 2019)

But: Be stars are not so strictly periodic.
See review by Rivinius *et al.* 2013.

2. Precessing jet

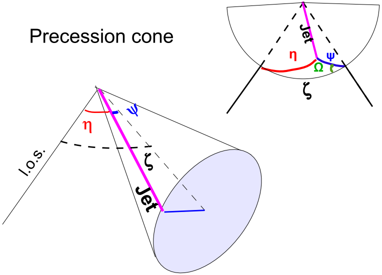

Figure 1 in Massi & Torricelli-Ciamponi (2014)

First rejected by Gregory *et al.* (1989)

Physical model reproduces observations:
Massi & Torricelli-Ciamponi 2014, A&A, 585, A123
Jaron *et al.* 2016, A&A, 595, A92

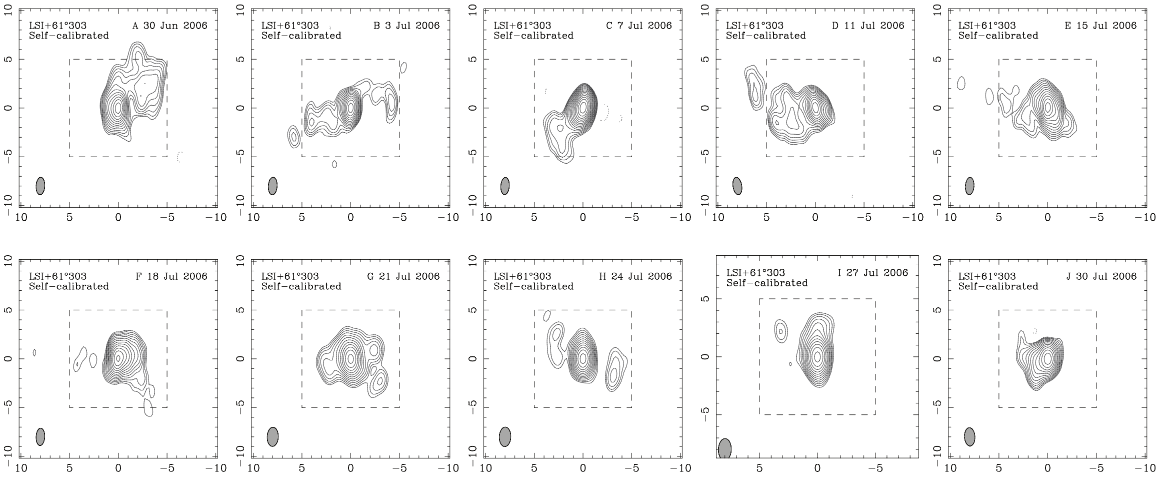

Figure: Detail from Fig. 1 in Massi, Ros, & Zimmermann 2012, A&A, 540, A142

$\Rightarrow$ Precession period $P_{\mathrm{precession}} \approx 27 - 28$ days (C.f. $P_{\mathrm{orbit}} \approx 26.5\,\mathrm{days} \neq P_{\mathrm{precession}}$)

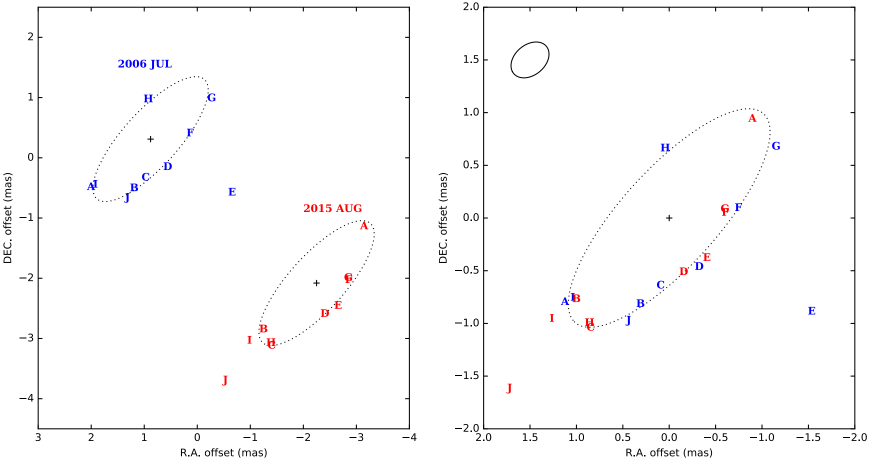

Figure 4. *Left-hand panel*: astrometric results of 2006 and 2015 VLBA observations, with parallax motions removed. Blue characters denote jet peaks in 2006, and red characters denote jet peaks in 2015. The reference coordinate (zero-point) is $02^{h}40^{m}31^{s}.6645$, $61^{d}13^{m}45^{s}.594$. *Right-hand panel*: same as left-hand panel, but with centres of the two ellipses overlaid. The solid ellipse in the top left corner indicates the scale of the orbit, with a semimajor axis of 0.22 mas (Massi et al. 2012).

$\Rightarrow P_{\text{precession}} = 26.926 \pm 0.005\,\text{days}$ Wu *et al.* 2018, MNRAS, 474, 3

Doppler boosting

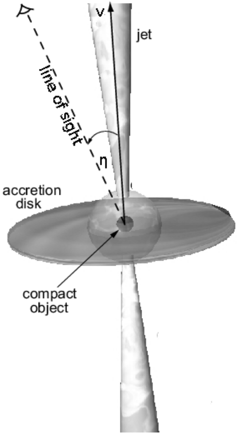

Observed flux amplified (attenuated) for approaching (receeding) jet with velocity v,

$$S_a = S_0 \left(\frac{1}{\gamma (1 - \beta \cos \eta)} \right)^{\kappa - \alpha} = S_0 \delta_a^{\kappa-\alpha},$$

$$S_r = S_0 \left(\frac{1}{\gamma (1 + \beta \cos \eta)} \right)^{\kappa - \alpha} = S_0 \delta_r^{\kappa-\alpha},$$

where $\beta = \frac{v}{c}$, $\gamma = \frac{1}{\sqrt{1-\beta^2}}$, and η is the angle between v and the line of sight.

Based on Fig. 1 in Reynoso & Romero 2009, A&A, 493, 1

Lomb-Scargle Periodogram

Radio:

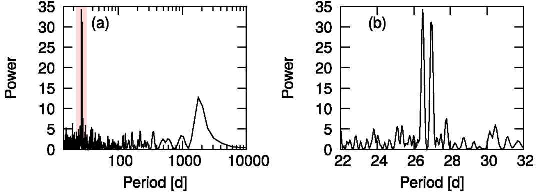

Jaron *et al.* 2018, MNRAS, 478, 1

Lomb-Scargle Periodogram

Radio:

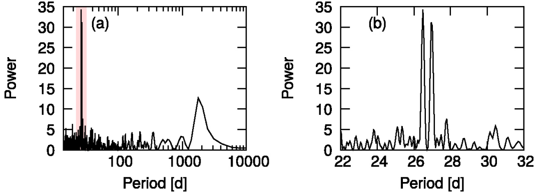

Jaron *et al.* 2018, MNRAS, 478, 1

X-rays:

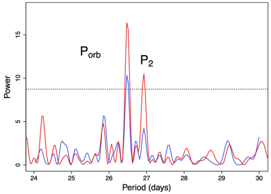

D'Aì *et al.* 2016, MNRAS, 456, 2

Lomb-Scargle Periodogram

Radio:

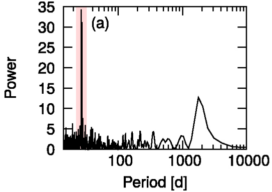

Jaron *et al.* 2018, MNRAS, 478, 1

X-rays:

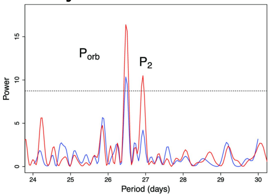

D'Aì *et al.* 2016, MNRAS, 456, 2

High-energy gamma-rays (*Fermi*-LAT):

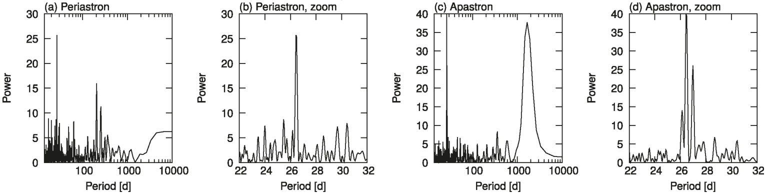

Jaron *et al.* 2018, MNRAS, 478, 1

Lomb-Scargle Periodogram

Radio:

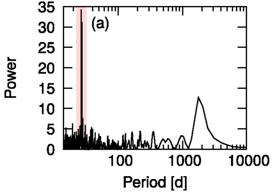

Jaron *et al.* 2018, MNRAS, 478, 1

X-rays:

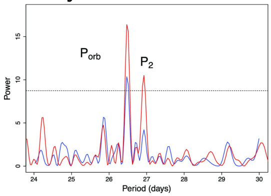

D'Aì *et al.* 2016, MNRAS, 456, 2

High-energy gamma-rays (*Fermi*-LAT):

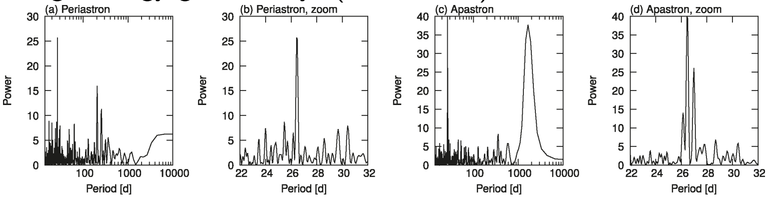

Jaron *et al.* 2018, MNRAS, 478, 1

Further publications on P_1 and P_2

Massi & Jaron 2013, A&A, 554, A105
Jaron & Massi 2014, A&A, 572, A105
Massi, Jaron & Hovatta 2015, A&A, 575, L9
Massi & Torricelli-Ciamponi 2016, A&A, 585, A123
Jaron, Torricelli-Ciamponi, Massi 2016, A&A, 595, A92

The long-term modulation is the beating between orbit and precession

Two close periods:

Orbit	$P_1 = 26.4960 \pm 0.0028\,\mathrm{d}$	Gregory 2002, ApJ, 575, 1
Precession	$P_2 = 26.926 \pm 0.005\,\mathrm{d}$	Wu *et al.* 2018, MNRAS, 474, 3

Interference: Beating (Massi & Jaron 2013, A&A, 554, A105)

$$\cos\omega_1 t + \cos\omega_2 t = 2\cos\left(\frac{\omega_1+\omega_2}{2}t\right)\cos\left(\frac{\omega_1-\omega_2}{2}t\right), \ \omega = \frac{2\pi}{P}$$

Envelope of interference pattern has period $P_{\mathrm{beat}} = 1659 \pm 22\,\mathrm{d}$
C.f. $P_{\mathrm{long}} = 1667 \pm 8\,\mathrm{d}$ by Gregory 2002, ApJ, 575, 1

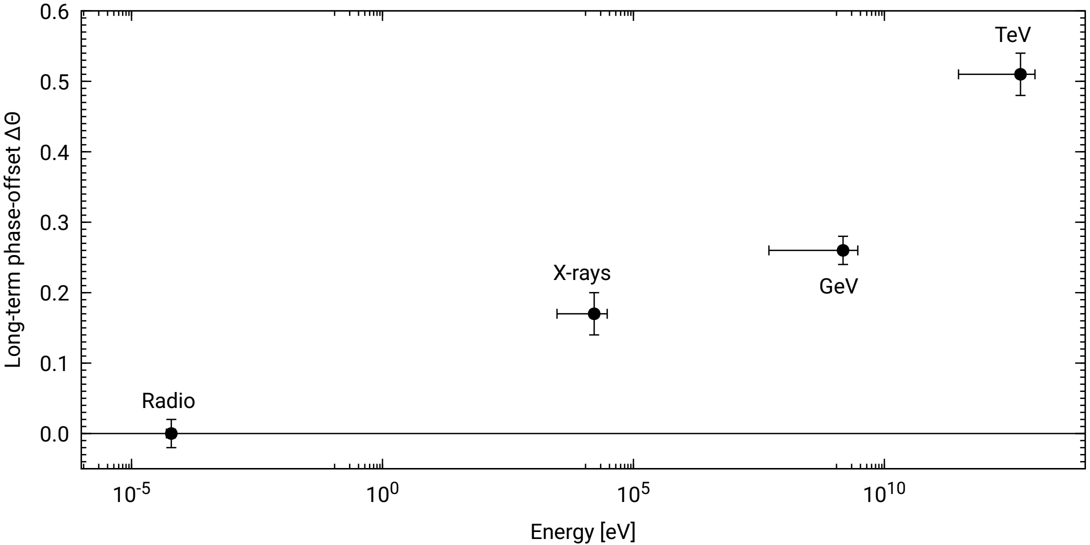

Jaron, Universe 2021, 7(7), 245

Reason for phase-offset in interference pattern

$$f_{\text{beat}}(t) = f_{\text{orb}}(t) + f_{\text{prec}}(t) = \cos 2\pi\left(\frac{t-T_0}{P_1}\right) + \cos 2\pi\left(\frac{t-T_0}{P_2} - \phi_{\text{mp}}\right)$$
$$\propto \cos 2\pi\left(\frac{t-T_0}{P_{\text{avg}}} - \frac{\phi_{\text{mp}}}{2}\right)\cos 2\pi\left(\frac{t-T_0}{2P_{\text{beat}}} + \frac{\phi_{\text{mp}}}{2}\right)$$

Precession profile phase-shifted by ϕ_{mp} $\Rightarrow$ Envelope of interference pattern shifted by $-\phi_{\text{mp}}$.

Explicitely observed for radio and GeV:

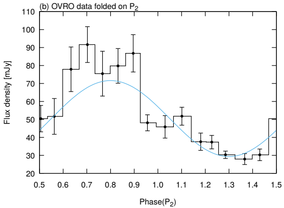

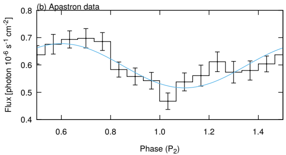

P_2: $\Delta\phi = -0.20 \pm 0.03$
P_{long}: $\Delta\phi = +0.26 \pm 0.03$

Jaron *et al.* 2018, MNRAS, 478, 1

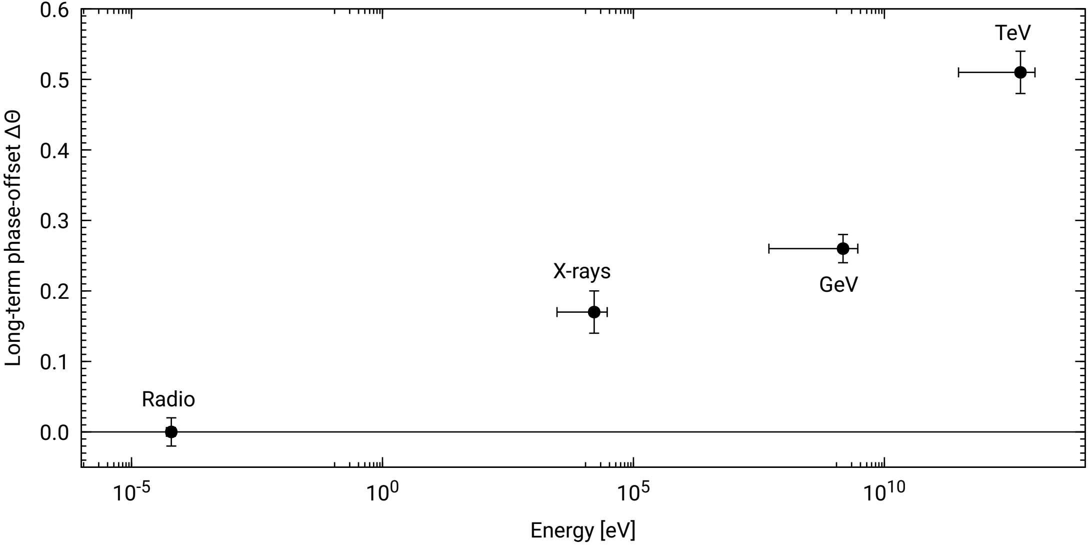

Jaron, Universe 2021, 7(7), 245

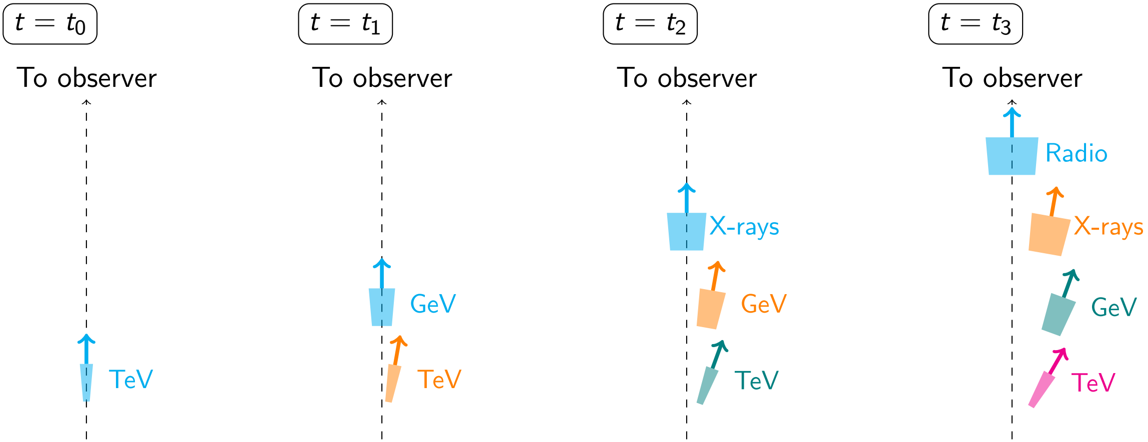

Jaron, Universe 2021, 7(7), 245

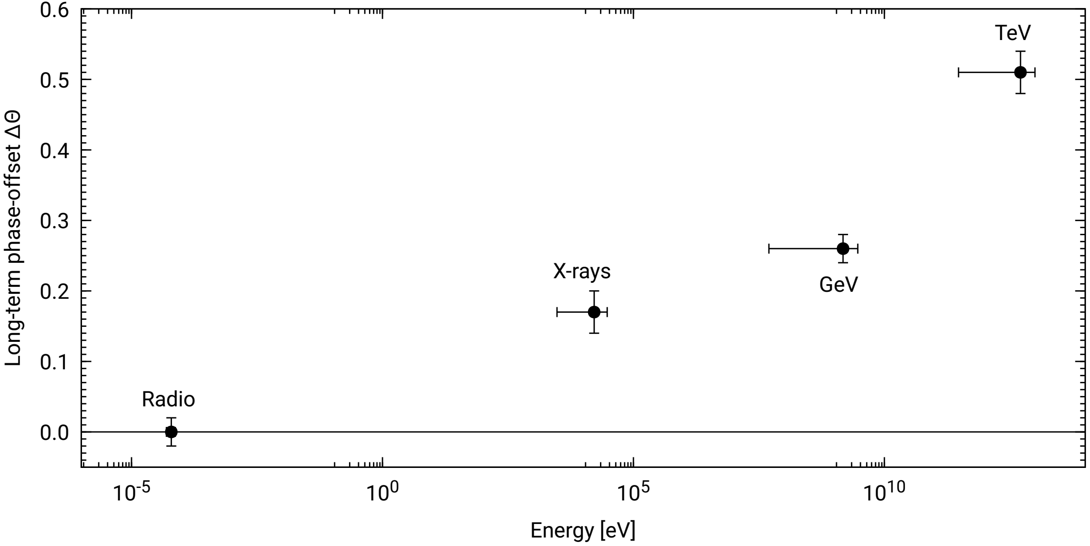

Jaron, Universe 2021, 7(7), 245

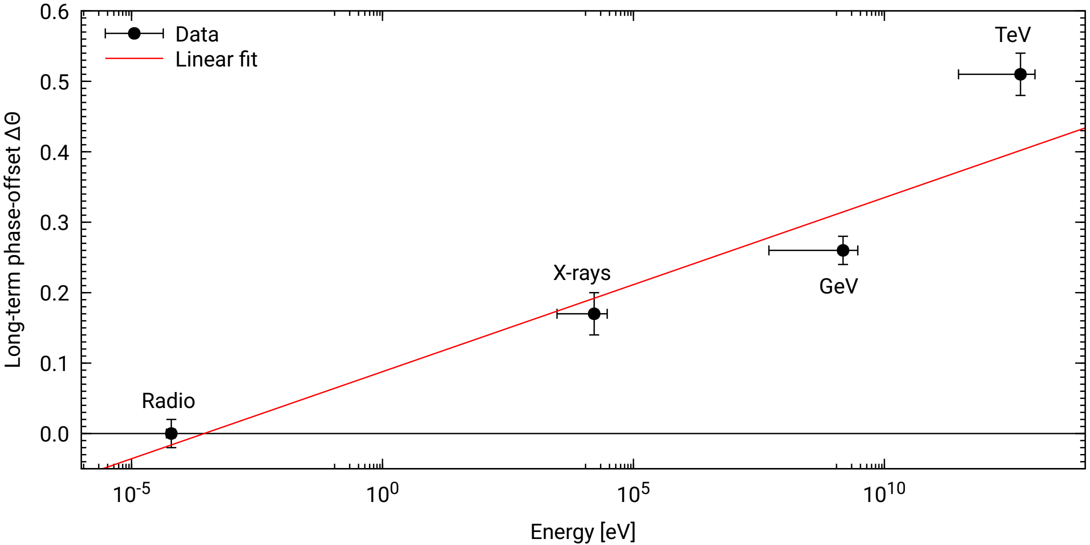

Jaron, Universe 2021, 7(7), 245

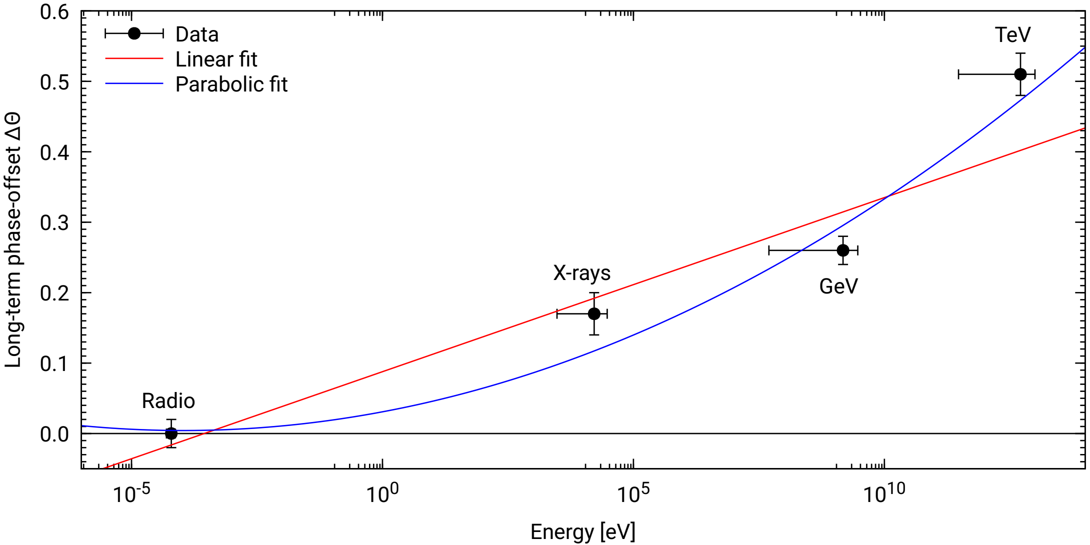

Jaron, Universe 2021, 7(7), 245

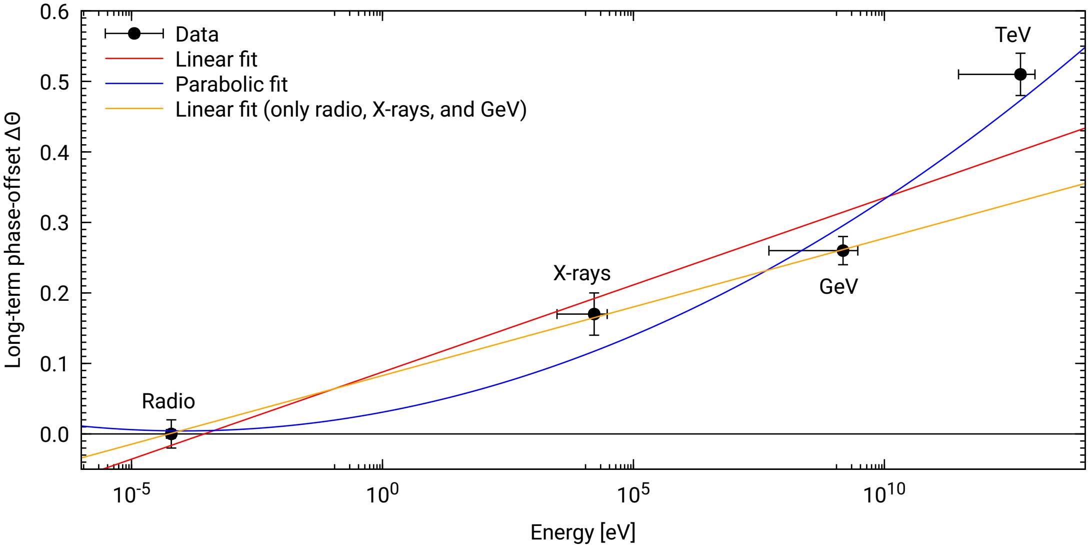

Jaron, Universe 2021, 7(7), 245

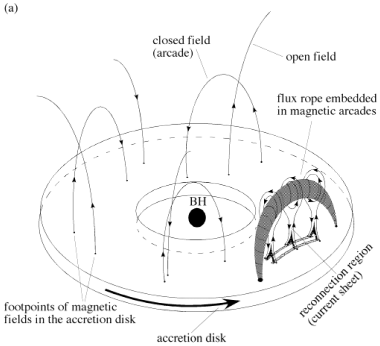

Fig. 1 a in Yuan *et al.* 2009, MNRAS, 395, 2183

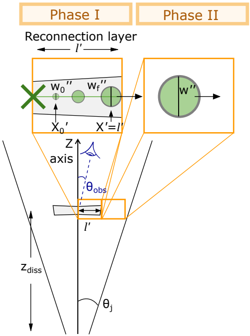

Fig. 1 in Petropoulou *et al.* 2016, MNRAS, 462, 3325

Magnetic reconnection can occur in the...

- disk Yuan *et al.* 2009, MNRAS, 395, 2183
- jet Petropoulou *et al.* 2016, MNRAS, 462, 3325; Sironi *et al.* 2016, MNRAS, 462, 48

In magnetic reconnection events the current sheet fragments into a chain of plasmoids that can be of different size and can be ejected with different timescales (minutes, hours, days).
Short-term variability observed: Sharma *et al.* (2021) ; Nösel *et al.* (2018) ; Jaron *et al.* (2017) ; Peracaula *et al.* (1997).

1. The binary system LS I $+61°303$ is variable and periodic across the electromagnetic spectrum.

1. The binary system LS I $+61^{\circ}303$ is variable and periodic across the electromagnetic spectrum.
2. A periodic long-term modulation pattern shows systematic phase-offsets with increasing energy.

1. The binary system LS I $+61^{\circ}303$ is variable and periodic across the electromagnetic spectrum.
2. A periodic long-term modulation pattern shows systematic phase-offsets with increasing energy.
3. Scenario: Lower energy emission originates downstream from higher energy emission in a precessing jet.

1. The binary system LS I $+61^{\circ}303$ is variable and periodic across the electromagnetic spectrum.
2. A periodic long-term modulation pattern shows systematic phase-offsets with increasing energy.
3. Scenario: Lower energy emission originates downstream from higher energy emission in a precessing jet.
4. Modification: The TeV emission is produced in magnetic reconnection events.

1. The binary system LS I $+61^{\circ}303$ is variable and periodic across the electromagnetic spectrum.
2. A periodic long-term modulation pattern shows systematic phase-offsets with increasing energy.
3. Scenario: Lower energy emission originates downstream from higher energy emission in a precessing jet.
4. Modification: The TeV emission is produced in magnetic reconnection events.
5. Continued long-term monitoring and at additional wavelenghts will help to better understand the physical processes in LS I $+61^{\circ}303$.

1. The binary system LS I $+61°303$ is variable and periodic across the electromagnetic spectrum.
2. A periodic long-term modulation pattern shows systematic phase-offsets with increasing energy.
3. Scenario: Lower energy emission originates downstream from higher energy emission in a precessing jet.
4. Modification: The TeV emission is produced in magnetic reconnection events.
5. Continued long-term monitoring and at additional wavelenghts will help to better understand the physical processes in LS I $+61°303$.

Thank you!